Water Production Rates and Activity of Interstellar Comet 2I/Borisov. Z. Xing[1,2], D. Bodewits[2], J. Noonan[3] and M. T. Bannister[4,5], [1]Department of Physics, Chong Yuet Ming Physics Building, The University of Hong Kong, Hong Kong SAR, China (zexixing@hku.hk) [2]Physics Department, Leach Science Center, Auburn University, Auburn, AL, 36830, USA [3]Department of Planetary Sciences, Lunar and Planetary Laboratory, University of Arizona, Tucson, AZ 85721, USA [4]Astrophysics Research Centre, School of Mathematics and Physics, Queen's University Belfast, Belfast BT7 1NN, United Kingdom [5]School of Physical and Chemical Sciences -- Te Kura Matū, University of Canterbury, Private Bag 4800, Christchurch 8140, New Zealand

Introduction: Extrasolar comets offer a glimpse into the building blocks, formation, and evolution of other planetary systems. Impacts by exocomets may significantly alter the atmospheres of exoplanets [1] or introduce species that could be conceived as biosignatures [2]. Interstellar comets might also furnish the exchange of volatiles and complex molecules between different planetary systems. With an eccentricity of 3.357, there is no question regarding the extrasolar origins of 2I/Borisov (Minor Planet Center; MPEC 2019-W50). At the time of its discovery, at 3 au from the Sun, the appearance of Borisov was that of a 'regular' comet, featuring a prominent tail and coma. Here, we report on our 3-month long monitoring campaign of 2I/Borisov with the Neil Gehrels-*Swift* observatory before and around its perihelion on Dec. 8.55 UTC.

Observations: In this study we used UltraViolet Optical Telescope (UVOT) [3] of The Neil Gehrels-*Swift* Observatory (*Swift*) [4] to determine water production rates and the dust content of 2I/Borisov. *Swift*/UVOT observed 2I/Borisov using its V (central wavelength 546.8 nm, FWHM 76.9 nm) and UVW1 (central wavelength 260 nm, FWHM 69.3 nm) filters for four times respectively on 2019 September 27, November 1, December 1 and December 21 UTC.

Mid Time	2019-09-27T08:52:40	2019-11-01:T19:52:26	2019-12-01T12:17:04	2019-12-21T12:52:31
$T-T_p$ (days)	-72.2	-36.7	-7.0	13.0
r_h (AU)	2.56	2.17	2.01	2.03
dr_h (km/s)	-23.54	-14.43	-3.00	5.48
Δ (AU)	3.10	2.42	2.04	1.94
S-T-O (°)	17.31	24.24	28.12	28.60
UVW1 T_{exp} (s)	8205	5487	5071	6346
V T_{exp} (s)	2712	1935	386	1937

Table 1 – Summary of the observing log. For the exposure time we only list the net exposure time of the stacked images, for which images contaminated by background stars were excluded.

Analysis: To increase the SNR of our images, we stacked the individual exposures within each of the four visits after discarding exposures contaminated by stars. The comet was clearly detected in the V co-added image of every visit (Fig.1), with a tail towards the anti-solar direction (Fig.1). In the UVW1 images of last three visits, this tail is mostly absent, and an extended coma can be clearly seen within a radius of ~100 000 km; at larger distances, background variations obscure the comet.

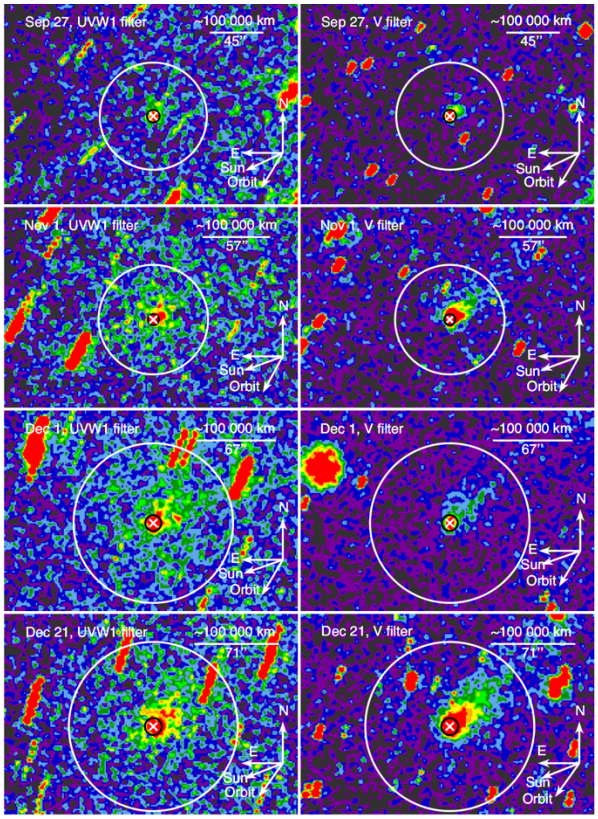

Fig. 1 – Co-added *Swift*/UVOT observations of 2I/Borisov (Left: UVW1; Right: V). The position of the comet nucleus is indicated by a white x-mark. White circles indicate photometric apertures used to measure water production rate and all have radii of 100 000 km. Black circles indicate apertures used to measure $A(\theta)f\rho$, with radii of 10 000 km for the last three visits and a larger radius of 12 000 km for the September visit. All panels have the same physical scale, and have been individually stretched linearly for optimal presentation, with north up, east to the left.

Dust content. The V-band mostly samples continuum reflected by the dust in the coma. We used the stacked images to measure the comet's V-band magnitudes and derive A(θ)fρ, a measure of the dust content in the coma [5]. We used circular apertures of a fixed radius of 10 000 km centered on the nucleus for the visits between November and December, and a slightly larger aperture of 12 000 km (5.3 pix) for the September visit. We calculated magnitudes m and used these to derive A(θ)fρ Finally, we normalized A(θ)fρ to a phase angle of 0 deg with the empirical phase function from D. Schleicher.

Water Production Rate. The UVW1 filter is well-placed to map fluorescent emission from the OH $A^2\,\Sigma^+ – X^2\,\Pi$ band between 280 and 330 nm [6]. To determine the flux of OH, we need to remove the continuum contribution to the UVW1 filter. For this, we developed an iterative process where we first assumed grey dust that reflects sunlight. We converted the resulting surface brightness profiles into a OH column density profiles using heliocentric velocity dependent fluorescence efficiencies [7], scaled by the comet's heliocentric distance squared r_h^{-2}. To determine water production rates, we compared our OH column density profiles with vectorial model calculations, and found that the continuum near the nucleus was oversubtracted owing to the reddening of the dust (top panel of Fig.2). We then empirically adjusted the continuum removal factor α (i.e. reddening) so that the column density profiles best matched the vectorial model distribution (top panel of Fig.2).

Results and Discussion:
We did not detect any OH on the first visit on Sep. 27. Between Nov. 1 to Dec. 1 water production rates increased gradually and appears to decrease rapidly after that. These results are in good agreement with those acquired by others. To further investigate the behavior of the comet's evolving activity, we calculated the required minimum active area corresponding to the water production rates using the sublimation model by [8], where we assume that every surface element has constant solar elevation. This maximizes the sublimation averaged over the entire surface, and results in a minimum total active area. Comparison between the result with the current tightest constraints from [9] implies that a significant fraction of the surface of Borisov is active.

Acknowledgments: We thank the *Swift* team for use of Director's Discretionary Time and for the careful and successful planning of these observations. This research has made use of NASA's Astrophysics Data System Bibliographic Services.

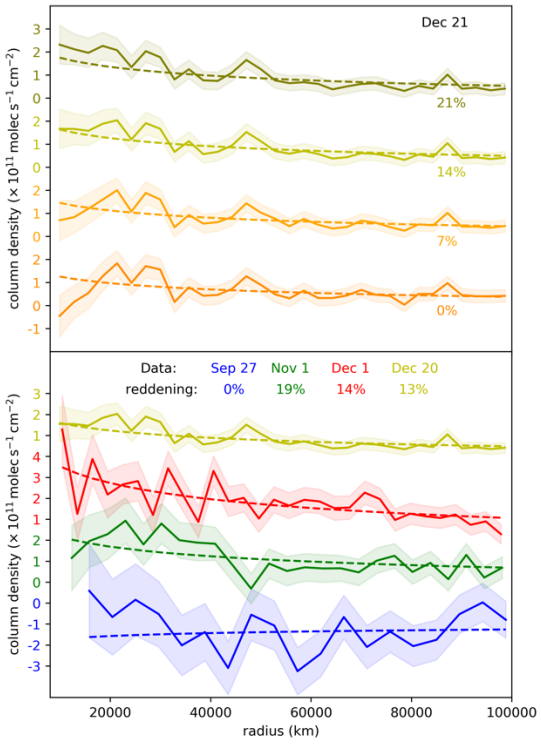

Fig. 2 – Top: Column density profiles with different continuum colors for the visit on Dec 21. Solid curves indicate column density profiles produced by removing scaled V-band images from observed UVW1-band images, adjusted for different levels of continuum reddening (% per 100~nm between between 260 and 547 nm). Dashed curves are vectorial model profiles scaled to match the measured curves. Bottom: Comparison of column density profiles for the 4 visits, same symbols are in the top panel.

References:
[1] Kral, Q. et al. (2018), MNRAS, 479, 2649.
[2] Seager, S. et al. (2016) Astrobiology, 16, 465.
[3] Roming, P. W. (2000) Proc SPIE.
[4] Gehrels, N. et al. (2004) ApJ, 611, 1005.
[5] A'Hearn, M. F. et al. (1984) 89, 579.
[6] Bodewits, D. et al. (2014) ApJ, 786, 48.
[7] Schleicher, D. G. & A'Hearn M. F. (1988) ApJ, 331, 1058.
[8] Cowan, J. J. & A'Hearn, M. F. (1979) Moon and Planets, 21, 155.
[9] Jewitt, D. et al. (2019) arXiv: 1912.05422.